Evidence that αC Region Is Origin of Low Modulus, High Extensibility, and Strain Stiffening in Fibrin Fibers

John R. Houser,[†△] Nathan E. Hudson,[†△] Lifang Ping,[‡] E. Timothy O'Brien III,[†] Richard Superfine,[†] Susan T. Lord,[‡] and Michael R. Falvo[†*]

[†]Department of Physics and Astronomy, and [‡]Department of Pathology and Laboratory Medicine, University of North Carolina at Chapel Hill, Chapel Hill, North Carolina

ABSTRACT Fibrin fibers form the structural scaffold of blood clots and perform the mechanical task of stemming blood flow. Several decades of investigation of fibrin fiber networks using macroscopic techniques have revealed remarkable mechanical properties. More recently, the microscopic origins of fibrin's mechanics have been probed through direct measurements on single fibrin fibers and individual fibrinogen molecules. Using a nanomanipulation system, we investigated the mechanical properties of individual fibrin fibers. The fibers were stretched with the atomic force microscope, and stress-versus-strain data was collected for fibers formed with and without ligation by the activated transglutaminase factor XIII (FXIIIa). We observed that ligation with FXIIIa nearly doubled the stiffness of the fibers. The stress-versus-strain behavior indicates that fibrin fibers exhibit properties similar to other elastomeric biopolymers. We propose a mechanical model that fits our observed force extension data, is consistent with the results of the ligation data, and suggests that the large observed extensibility in fibrin fibers is mediated by the natively unfolded regions of the molecule. Although some models attribute fibrin's force-versus-extension behavior to unfolding of structured regions within the monomer, our analysis argues that these models are inconsistent with the measured extensibility and elastic modulus.

INTRODUCTION

Fibrin is a structurally hierarchical biomaterial with remarkable mechanical properties (1). Fibrin fibers have extraordinary elasticity and extensibility (2–6), and the gels they constitute exhibit highly nonlinear elasticity (7–10). There is increasing appreciation of the hierarchical design found in biomaterials like fibrin, that give rise to their remarkable properties (11–13). Understanding the underlying design requires attention to each organizational level within this hierarchy. Fibrin presents an interesting case of a biomaterial with a complex hierarchical structure. The monomer itself is a very large molecule at 340 kDa, with multiple domains including globular regions, coiled-coils, and unstructured regions (1,14,15). The monomers polymerize through a variety of distinct interactions to form protofibrils. The protofibrils in turn laterally aggregate to form the fibrin fiber. The fibers branch and coalesce to form a three-dimensional network, often called a fibrin gel. The fibrin network is stabilized by isopeptide bonds between monomers, whose addition is catalyzed by the active transglutaminase factor XIII (FXIIIa). The emergent mechanical properties of the fibrin gel are a function of the mechanical properties of the components of each hierarchical level—monomer, protofibril, fiber, and network—and the architectural transitions between one level and the next—monomer-monomer interactions, lateral aggregation, and branching.

The macroscopic mechanical properties of the highest rung in this structural hierarchy, fibrin gels, have been studied for decades going back to the pioneering work of Ferry and co-workers (16–18) and others (19–21). These studies showed that fibrin networks exhibit highly nonlinear elasticity manifested in strain stiffening behavior (7–9) and negative normal stress (10). Macroscopic studies have also long established the importance of FXIIIa-induced ligation in stabilizing clots (1). Ligated clots show a much higher storage modulus, a lower loss modulus, and are more resistant to lysis by proteases (1,22). FXIIIa catalyzes formation of isopeptide bonds between γ-regions and α-regions of the monomer resulting in $\gamma-\gamma$, $\alpha-\alpha$, and $\gamma-\alpha$ interactions (23,24). The ligated $\gamma-\gamma$ and $\alpha-\alpha$ interactions, in particular, have been determined to contribute, independently, to the increased stiffness of whole clots (23). At the molecular-scale of the spatial hierarchy, recent atomic force microscope (AFM) force spectroscopy measurements evaluated the mechanical properties of the molecule itself. These studies focused on the coil-coil (25,26) and the globular γ-region (27,28) and revealed mechanisms that may play a role in larger scale mechanical deformation. The stage in the hierarchy that has received the least attention is arguably the most important: the individual fiber.

We recently reported that individual fibrin fibers exhibit extraordinary extensibility with an elastic regime in excess of a strain of 1.0, and strains at breaking of up to 3.0 (strain is defined here as fiber extension divided by original fiber length; a strain of 1.0 is a doubling of the fiber length) (5,6). Four important and related questions emerge from this work:

Submitted May 27, 2010, and accepted for publication August 23, 2010.

△John R. Houser and Nathan E. Hudson contributed equally to this work.

*Correspondence: falvo@physics.unc.edu

Editor: Denis Wirtz.

0006-3495/10/11/3038/10 $2.00

doi: 10.1016/j.bpj.2010.08.060

1. What are the full force extension characteristics of the fibrin fiber?
2. Is fibrin an elastomeric fiber?
3. What are the molecular origins of extensibility?
4. How does FXIIIa ligation affect stiffness and extensibility?

Along with very high extensibility, fibrin has a relatively low modulus (1–10 MPa range) and exhibits strain-stiffening behavior above strains of 1.0, as we have recently reported (2) and as Liu et al. (3) showed in their recent evaluation of the viscoelastic properties of fibrin fibers. These properties place fibrin squarely in the category of biomaterials such as elastin, resilin, and spider silk (29,30). This result is somewhat surprising, given fibrin is predominantly a structured globular protein which polymerizes into ordered semicrystalline arrangements in fibers (31). In contrast, elastomeric protein structures consist primarily of disordered networks of natively unfolded polypeptides with randomly distributed covalent cross-links (32). We present force-versus-extension data on fibrin fibers with and without FXIIIa ligation, and show fibrin fibers have relatively low elastic moduli and exhibit pronounced strain stiffening. We present a mechanical model of the fibrin fiber consisting of an ordered network of wormlike chain segments. The success of this model in fitting our force-versus-extension data suggests that fibrin's elasticity is entropic in origin, and that the observed stiffness and extensibility have their origins in unstructured regions of the protein.

MATERIALS AND METHODS

We used an AFM on top of an inverted epifluorescence light microscope to manipulate individual fibrin fibers (4,6). Fibrin fibers were polymerized on micron-sized optically transparent, patterned ridges made by microcontact printing ultraviolet curable optical adhesive (Norland Optical Adhesive 81; Norland Products, Cranbury, NJ). We manipulated fibers that were suspended across channels and adhered at each end to the ridge tops (see Fig. 1). We used nanoManipulator (3rdTech, Durham, NC) software to collect data and control the AFM tip which was carefully positioned next to a suspended fiber (several microns above the channel floor) and moved at a constant height in a trajectory perpendicular to the fiber axis. For the stress-versus-strain data depicted in Fig. 2 and later in Fig. 4, force data was converted to stress by taking the calibrated force data and dividing by cross-sectional area of the fibrin fiber as determined by AFM imaging (AFM measured fiber diameter which was converted to area assuming circular cross section). In all experiments, we used recombinant human fibrinogen produced in Chinese Hamster Ovary cells (33,34). We assessed purity and homogeneity of this material through sodium dodecyl sulfide-polyacrylamide gel electrophoresis and immunoblot analyses. Further details concerning our Materials and Methods are included in the Supporting Material.

RESULTS AND DISCUSSION

Single fiber stress versus strain

We prepared fibrin samples on micropatterned substrates with individual fibers suspended across channels (experimental geometry depicted in Fig. 1). The sequence in

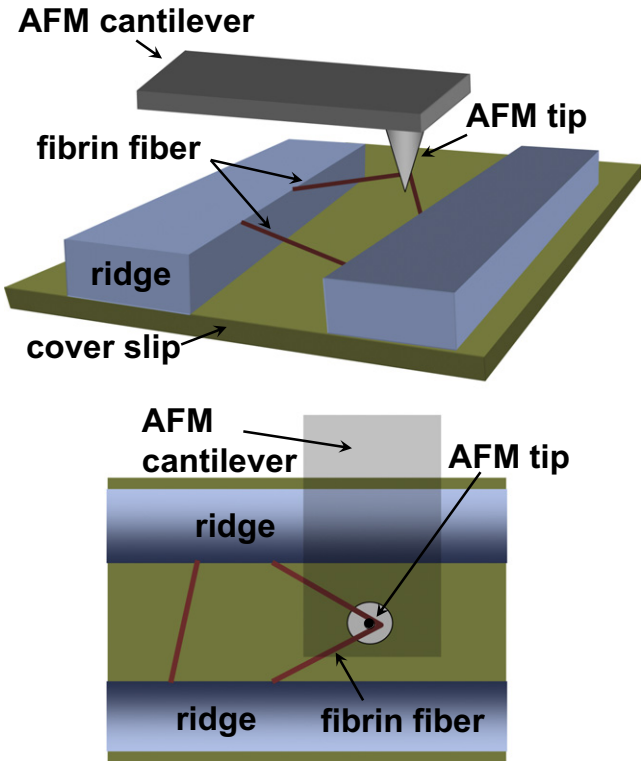

FIGURE 1 Setup for single fiber and network stretching experiments. Suspended fibrin fibers are labeled with fluorescent beads and then stretched with the AFM tip. Movies of the stretching are taken from below with epifluorescence imaging.

Fig. 2, *A–D*, depicts an AFM measurement of a single fibrin fiber stretched to the point of failure. The raw AFM force and position data were converted into fiber tensile strain and stress (see Materials and Methods). Typical stress versus strain data for both FXIIIa ligated (*red*) and unligated fibers (*blue*) are depicted in Fig. 2 *E*, while Fig. 2 *F* shows their strain-dependent tangent moduli (the slopes of the stress versus strain curves in Fig. 2 *E*). At strain <1.0, both fibers had a low and constant modulus. Above strain of 1.0, the fibers showed strain-stiffening behavior. Both fibers exhibited roughly a 10-fold increase in stiffness between low and high strain. The bar plot in Fig. 3 depicts the average differential modulus at discrete strains for fibers with and without FXIIIa ligation. The FXIIIa-ligated fibers had an average elastic modulus of 2.1 ± 0.3 MPa at 0.25 strain rising to an average of 9.8 ± 1.2 MPa at failure. The unligated fibers showed 1.1 ± 0.2 MPa at 0.25 strain rising to 6.9 ± 1.3 MPa at failure. As a way of quantifying strain stiffening, we calculated the average ratio of maximum modulus to the modulus at 0.25 strain; the ligated fibers stiffened by a factor 6.2 ± 0.8, and unligated fibers stiffened by a factor 7.7 ± 1.5.

In situ measurements

Determination of the stress-versus-strain behavior of fibers yields intensive materials parameters such as elastic

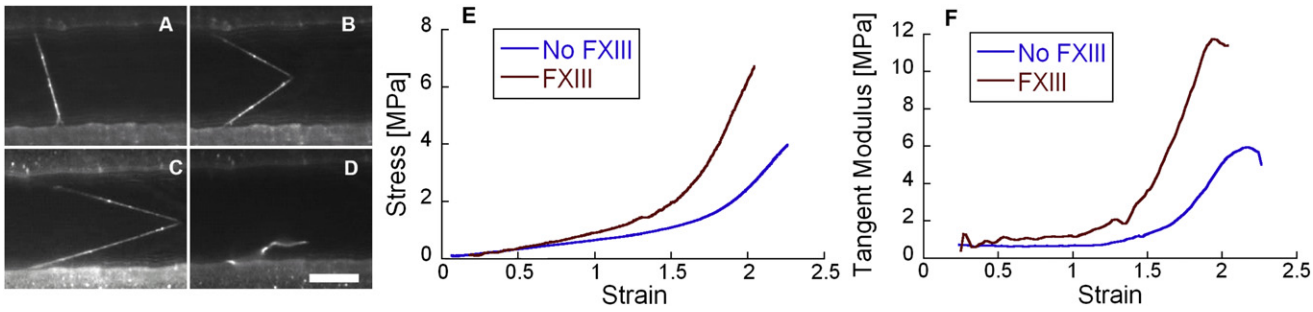

FIGURE 2 Stress-versus-strain plots of individual fibrin fibers. (*A–D*) AFM manipulation of a fibrin fiber suspended over micropatterned channel. The AFM tip (not visible) was brought in contact with a suspended fiber and stretched (*B* and *C*) to the point of failure (*D*). Scale bar = 10 μm. (*E*) Representative stress-versus-strain data of individual fibers with and without FXIII ligation. Both fibers show relatively linear behavior up to strain just above 1.0 followed by significant stiffening. (*F*) Tangent modulus illustrating the strain-dependent stiffness. These traces were found by numerically differentiating the traces in panel *E*. At high strains just before failure, the tangent moduli levels off and drops, indicating an end to stiffening. It is not clear this reflects the intrinsic properties of the fiber or is a result of slippage at constraint points.

modulus by normalizing the raw-force-versus-elongation data by the length and diameter of the fibers. This allowed comparison of the stiffness of different fibers over many experiments. We estimated the fiber cross-sectional area by using the AFM to measure the diameter of the fiber on the ridge. In calculating stress, we assumed that the fiber cross section is circular, that the fiber diameter on the ridge surface is equivalent to the suspended fiber diameter, and that the diameter is constant over the suspended length. A comparison of the full stress-versus-strain behavior from one experiment to another also requires comparing data from different AFM tips and force calibrations, which adds additional uncertainties.

To address these uncertainties in comparing ligated to unligated fibers, and to corroborate the stress-versus-strain data, we measured the relative change in stiffness of individual fibrin fibers before and after FXIIIa ligation in situ (Fig. 3). Results of a Western blot indicating successful ligation is shown in Fig. 4 (see Materials and Methods). These measurements provided direct comparisons of fiber stiffness with and without ligation in the same fibers, thus obviating the need for geometrical normalizations or force calibration. Fibrin was prepared on structured surfaces without ligation, then stretched with the AFM. These initial stretches corresponded to strains of 0.40 or less in order to maintain mechanical reversibility. FXIIIa was then added to the sample and the same fiber was stretched again. Fig. 5 shows representative data revealing increased stiffness with addition of FXIIIa. We observed an increase in stiffness after ligation by FXIIIa in all eight fibers we measured; the average increase was 80%, in agreement with an increase of 90 ± 44% obtained from the stress versus strain measurements at strain of 0.25 (Fig. 3). These

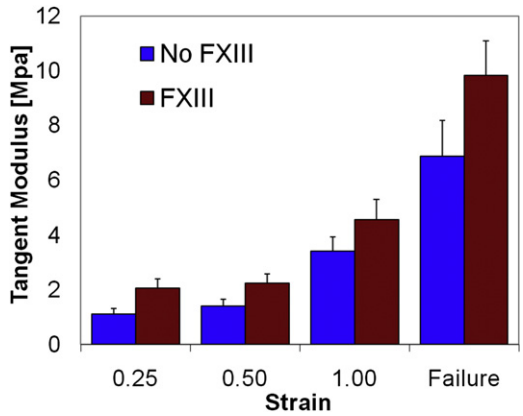

FIGURE 3 Average tangent modulus at discrete strains for ligated ($N = 14$) and unligated ($N = 14$) fibers. At 0.25 strain, the ligated fibers have an elastic modulus of 2.1 ± 0.3 MPa whereas the unligated have a modulus of 1.1 ± 0.2 MPa ($P < 0.003$). The average modulus rises to 9.8 ± 1.2 MPa for ligated and 6.9 ± 1.3 MPa for unligated fibers ($P < 0.05$).

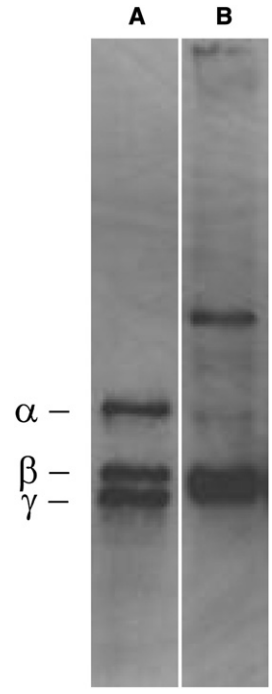

FIGURE 4 Western blot of fibrin showing α-, β-, and γ-bands without FXIIIa (*A*) and α-, β-, and γ-γ dimer after ligation with FXIIIa (*B*).

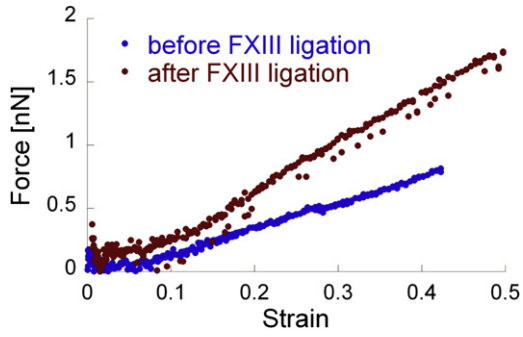

FIGURE 5 In situ fiber stiffness measurements. Fiber stiffness before (*blue*) and after (*red*) FXIII ligation.

results show that FXIIIa acts directly on the mechanical properties of the fiber itself; ligation more than doubles the fiber stiffness. Our results are also consistent with low strain thermal noise spectrum measurements taken on fibers in clots (35).

Model

To interpret the force-versus-extension data, we developed a model of the mechanics of fibrin fiber extension. Fig. 6 shows the structure of the fibrin monomer (6, *A* and *B*), and our mechanical model of a fibrin fiber consisting of an ordered array of fundamental mechanical units (Fig. 6, *D* and *E*). Each fundamental unit has an unstructured portion modeled mechanically as a wormlike chain (WLC) and a structured portion modeled as a Hookean spring. Previous reports agree that the extreme extensibility of the fibrin fiber reflects properties of the fibrin monomer. These reports suggest that an unfolded segment in the molecule is critical: either a natively unfolded region such as the αC domain (4) or a force-unfolded region such as the coiled-coil (25,36) or the γ-domain in the D region (28).

In any case, a large portion of the monomer's structured architecture will remain folded and is represented by the stiff spring. Because this spring represents the structured globular regions of the protein, its stiffness is expected to be several orders-of-magnitude higher than the unstructured region, and will not contribute significantly to the extension of the fiber (see the Supporting Material). Our force-extension model assumes that fiber extension is accommodated only by the unstructured region, which we model as a WLC. We have not explicitly included unfolding as a mechanism of extension in our model. Unfolding may be occurring, but our analysis shows it is unlikely until very high strain. Our force-versus-extension data also shows no signatures or features indicative of abrupt structural changes within the fiber. Our model is intended to present the simplest explanation of fibrin fiber extensibility that is consistent with what is known about fibrin fiber structure, the magnitudes of protein unfolding force thresholds, and the form of our force-versus-extension data.

Fig. 6 *C* depicts fibrin fiber structure in cartoon form, and a candidate model for fibrin extension. The dashed vertical lines in the upper cartoon of Fig. 6 *C* indicate the 22.5 half-stagger periodicity within the fiber that has been seen in numerous transmission electron microscope studies (31,37). The model depicts protofibrils laterally aggregated through αC interactions. The αC domains (*blue*) accommodate the majority of the fiber strain and are represented in the mechanical model (Fig. 6, *D* and *E*) by the WLC. As the cartoon of the strain fiber indicates, the αC regions can accommodate tensile strain, and act as springs in series within this proposed model, while also acting as lateral tethers between protofibrils. As the fiber is strained, these tethers align along the fiber axis and act as series connections between the stiffer protofibrils. The protofibril lengths depicted within this cartoon are relatively short for purposes of clarity, but are not inconsistent with published studies of protofibril lengths (38–40).

A WLC model has successfully described the force-extension behavior of DNA, intrinsically unstructured polypeptides, and force-unfolded proteins (41–46). The WLC is an idealized nonself-interacting flexible chain undergoing thermal fluctuations along its contour. The force of extension of the WLC is mediated entirely by entropic elasticity. Though this model has primarily been used to describe single-molecule force spectroscopy data, we apply it here, in scaled form, to a full fibrin fiber. The form of the force-versus-extension for a WLC in the Marko-Siggia form (46) is

$$F(\Delta l) = \frac{k_B T}{l_p}\left[\frac{1}{4}\left(1-\frac{\Delta l}{l_c}\right)^{-2} - \frac{1}{4} + \frac{\Delta l}{l_c}\right], \qquad (1)$$

where Δl is extension ($L - L_0$), k_B is the Boltzmann constant, T is temperature, l_p is persistence length, and l_c is the contour length. We note our use of Δl in Eq. 1, rather than end-to-end length as is appropriate for a single random coil polymer chain. In our case, we assume the relaxed length of the fiber segment, L_0, is due entirely to the structured portions of the monomer; the unstructured portion only contributes appreciable length to the fiber as it extends. In reality, the unstructured domains may contribute a small percentage to the unstretched fiber length, but we assume this contribution is negligible.

We model the force-extension behavior of the fundamental mechanical unit (Fig. 6 *D*) as a WLC (Eq. 1). The whole fibrin fiber is modeled by M identical fundamental units in series and N of these chains in parallel (Fig. 6 *E*). A chain with M identical WLCs linked in series behaves as a WLC with a contour length equal to M times the contour length of the primitive unit:

$$L_c = M * l_c. \qquad (2)$$

Substituting Eq. 2 into Eq. 1 yields the force extension relation for a series of M WLCs,

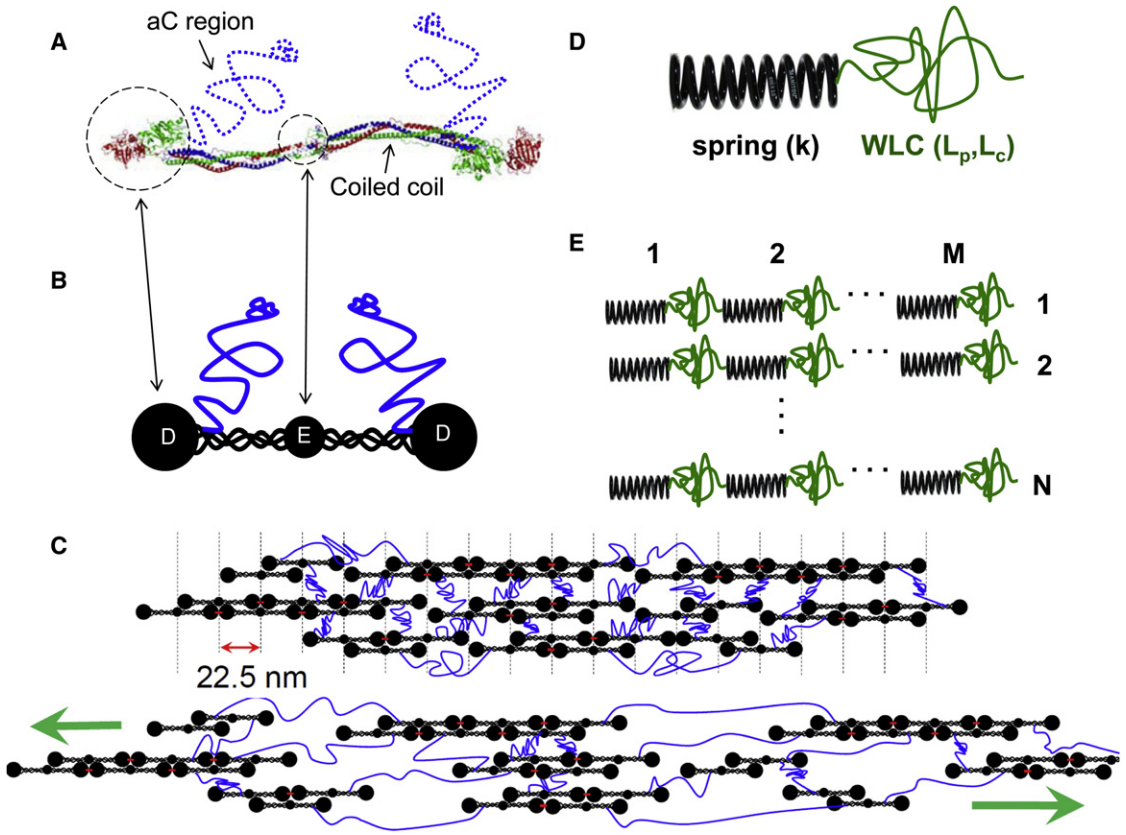

FIGURE 6 Fibrin structure and corresponding mechanical model. (*A*) Crystal structure of fibrinogen. The α-, β-, and γ-polypeptides in blue, green, and red respectively, with a cartoon of the C-terminus region of the α-chain (in *dashed blue*). (*B*) Cartoon depiction of the fibrinogen. (*C*) (*Upper model*) Simplified fibrin fiber structure. Intraprotofibril FXIII-induced covalent interactions (*red dashes*). Protofibrils are connected through αC region interactions (αC regions in *blue*). We note that this picture is simplified for clarity. In a real fiber, each monomer has two αC regions extending. Lines (*blue*) spanning protofibrils represent αC/αC interactions. Though the figure suggests only pairwise αC interactions, it is known that αC regions typically form interactions with multiple other αC regions. (*Dashed vertical lines*) The 22.5-nm half-stagger periodicity within the fiber that is evidenced by banding in numerous TEM studies. (*Lower model*) Stretching of the fiber under stress. This cartoon depicts a model of one potential mechanism of extensibility. In this case, the αC domains, though linking protofibrils laterally, accommodate the tensile strain induced by applied force (*green arrows*). The stiff protofibrils, within this model, are represented by the stiff springs and accommodate little of the strain. (*D*) Simple mechanical model of the fibrin monomer. The linear spring (*black*) represents the stiff structured portion of the monomer (spring constant k). The random coil (*green*) represents the unstructured portions of the protein. These could be either those regions natively unfolded (αC domain) or any mechanically unfolded region of the protein such as the coiled-coil or portion of the D region. The WLC force-versus-extension relation is parameterized with persistence length, L_p, and contour length, L_c. (*E*) Simplified mechanical model of the fibrin fiber. There are M monomers in series and N single monomer chains in parallel. The model includes no lateral interactions because they have no relevance to uniform tensile stretching.

$$F_{M,1}(\Delta L) = \frac{k_B T}{l_p}\left[\frac{1}{4}\left(1-\frac{\Delta L}{M * l_c}\right)^{-2} - \frac{1}{4} + \frac{\Delta L}{M * l_c}\right], \quad (3)$$

where ΔL is the extension of the entire fiber. The force of N WLCs in parallel is N times the force of the individual WLCs,

$$F_{M,N}(\varepsilon) = N * F_{M,1} = N * \frac{k_B T}{l_p}\left[\frac{1}{4}\left(1-\frac{\varepsilon}{(M * l_c)/L_0}\right)^{-2} - \frac{1}{4} + \frac{\varepsilon}{(M * l_c)/L_0}\right], \quad (4)$$

where here we normalize the extension, ΔL, and contour length, $M^* l_c$, to the original fiber segment length, L_o, to produced force as a function of strain ($\varepsilon = \Delta L/L_0$). Because of the ordered arrangement of monomers within our fibrin fiber model, the force extension relation for the full fiber (Eq. 4) is a scaled version of the single WLC relation with the persistence length l_p and contour length l_c replaced with l_p/N and Ml_c, respectively.

As Fig. 7 shows, the scaled WLC equation (Eq. 4) does a very good job of fitting force-versus-strain data for both the FXIIIa ligated and unligated fibers. The fitting parameters obtained are the scaled persistence length (l_p/N) and the scaled contour length (Ml_c/L_0). Both parameters provide insight into the molecular origins of fibrin's strain accommodation. To tease out the molecular parameters l_p and l_c, an estimate is made for M and N based on the geometry of the fiber determined by AFM of fibers on the ridges for

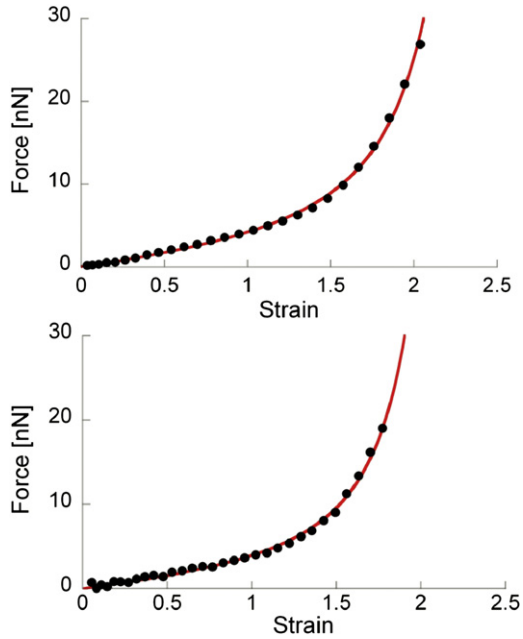

FIGURE 7 Force-versus-strain data (*black circles*) for unligated fiber (above) and ligated fiber below (5% of data points shown for clarity). (*Red curve*) Fit of Eq. 4.

diameter and fluorescence microscopy for the length. The number, N, is found by taking the ratio of the cross-sectional area of the fibrin fiber to the estimated cross-sectional area of a monomer (or the ratio of the squares of the diameters). Using 3–7 nm as a rough estimated range for the effective individual monomer diameter—corresponding to 200–1100 monomers in parallel for a 100-nm fiber (see the Supporting Material)—we obtain an average persistence length value of 0.1–0.6 nm. This number is intended to be taken as an order-of-magnitude benchmark to compare with results from other single-molecule force spectroscopy studies. Experimental persistence lengths for polypeptides fall in the range of 0.4–1.5 nm (25,42,47,48).

The second fitting parameter (Ml_c/L_0) describes the effective contour length of the fiber as a strain. L_0 is simply M times the original length of the monomer ($L_0 = Ml_o$)—for our fibers, L_o is typically 10 μm—and l_o is 45 nm, yielding $M = 220$ monomers in series. Substituting, the fitting parameter simplifies to (l_c/l_o). This is a scaled contour length that expresses the contour length of the unstructured portion of the monomer as a fraction of the original monomer length, l_o. We obtained a scaled contour length of 2.5 $\pm$ 0.4; at full extension of the unstructured portion of the monomer, the additional extension is 2.5 times the original length (and therefore the end-to-end length is 3.5 times the original end to end distance). For a monomer of 46 nm, this yields an additional length of ~115 nm. This length corresponds to 320 residues responsible for the WLC-like extension of the monomer, which, when split between the two identical sides of the fibrin monomer, yields 160 residues. The tethered αC region contains nearly 400 amino acids, at least 200 of which are known to be part of an unstructured region and could easily account for this additional length. An unfolded portion of the D region of the protein could also account for this additional length. Unfolding and completely extending both coiled-coil regions leads to 46-nm extra length (25), accounting for less than half of the extension. We found no statistically significant difference between FXIIIa ligated and unligated fibers in either the persistence length ($p > 0.20$) or the contour length ($p > 0.05$) parameters.

Does the αC connector region mediate fibrin's initial extensibility?

The αC region has been identified as a potential source of fiber extensibility in several recent publications (2–5,49). In a recent study, we demonstrated that fibrin extensibility is correlated to the length of the αC connector region in the fibrin monomer (4). The longer the length of the unstructured region, the longer the fiber was able to extend. For the αC regions to play a key role in the elastic modulus and extensibility of fibrin, they must be arranged within the fiber such that they make series connections (longitudinal) between protofibrils in addition to parallel (lateral) connections. The conventional picture of fibrin structure is that the αC regions connect in a lateral arrangement. However, work by Hantgan and Ferry, among others (38–40), has shown that protofibrils have a distribution of lengths varying from a few monomers up to 20 or so in standard polymerization conditions. Given the protofibrils are relatively short—a few hundred nm at most, as compared to the whole fiber which is tens of microns long—the interprotofibril connections must be crucial to supporting tensile forces. The αC regions are therefore likely to play a role as springs-in-series with the stiffer protofibrils (See Fig. 6 *E*). This view is consistent with our WLC-in-series model for fibrin extension and is generally consistent with the observed low modulus and high extensibility. However, this model strongly argues that the series αC connections give rise to a significant fraction of the total extension of the fiber.

Another important piece of the experimental evidence that is relevant to this question is the stiffening of the fiber with FXIII ligation. The fibrin monomer has known ligation sites within its γ-domains and its αC region (23,50). Within a model in which coiled-coil domain unfolding leads to fibrin's extensibility, and FXIII ligation only strengthens already existing γ-γ contacts (intraprotofibril interactions), it is hard to construct a scenario in which FXIIIa ligation would result in fiber stiffening. An increase in fiber strength—a higher tensile stress before failure—would be expected, but not stiffening. Instead, stiffening suggests the mechanisms of extension are becoming more restricted through FXIIIa ligation. Addition of new constraints on conformational freedom are required to provide this, and

we believe the most obvious places this could happen are in the interprotofibril αC connections. The αC region is known to have multiple sites that can form dipeptide bonds through FXIIIa ligation. The αC domains also interact noncovalently, independent of FXIIIa ligation (51). Like in a polymer gel, where increased cross-link density results in a stiffer material, additional covalent αC connections facilitated by FXIIIa would stiffen the interprotofibril mechanical linkages. Within our model, this would effectively reduce the average contour length of the constituent WLCs. Our fits to the force extension curves did not indicate clear change in the contour length fitting parameter, though we did observe stiffening of fibrin fibers with FXIIIa ligation. This could be due to incomplete ligation of the αC chains by FXIIIa in our reaction. Recent work by Liu et al. (3) showed that full αC ligation reduces the extensibility of the fiber, reducing the contour length. Further refinement in the force-versus-extension data as well as the WLC-in-series model may be required to tease-out subtle changes in the effective contour length of the αC upon FXIIIa ligation.

Coiled-coil unfolding

A 2007 force spectroscopy study of oligomers of fibrinogen showed compelling evidence of coiled-coil unfolding. In these studies, the applied force was necessarily transferred through the D region, coiled-coil, and E region, eliminating any contribution of the unstructured αC region. Thus, although these studies provide evidence that the coiled-coil is unfolding, it is not clear that the data are relevant to the stretching of physiological fibrin fibers, which are polymers with many parallel and series connections between monomers. More recently, a two-state model for fibrin extensibility has recently been proposed by Brown et al. (36) as part of an impressive multiscale study of large fibrin networks. This model assumes that unfolding of the coiled-coil region mediates fibrin's extensibility. In the model, the coiled-coils can be in two states: 1), the folded state where their stress-strain behavior is linear; and 2), the unfolded state where the coil is unfolded and behaves like a wormlike chain at high extensions (52). The distribution of folded and unfolded monomers is governed thermodynamically by the unfolding energy barrier and the distance between the energy wells of the folded and unfolded states.

This model is appealing in that it meshes well with the conventional view of fibrin structure in which the tensile force is supported completely through γ-γ contacts within the protofibrils with the coiled-coils acting as springs in series. However, the coiled-coil mediated extensibility model has difficulty accounting for the full stress-strain behavior of the fibrin fiber presented here and in other publications (2,3). We attempted to apply the two-state coiled coil model of Brown et al. (36) to our fibrin fiber force extension curves. The model fitting parameters required to match our experimental data were nonphysical (e.g., persistence lengths in the few pm range). Reasonable fitting also required a pre-unfolding coiled-coil stiffness in the 1–10 MPa range. Biomaterials whose extensibility is known to be mediated by coiled-coil unfolding, including myosin, egg capsule (53), and intermediate-filament-based materials such as keratin (54), vimentin (55,56), and others, all show a characteristic force-versus-extension signature that includes three force regimes: an initial stiff regime ranging from 150 to 1000 MPa corresponding to the unfolding of the hydrogen-bond-mediated coiled coil, a softer regime corresponding to the extension of the uncoiled peptide chain, and a second stiffening regime where the uncoiled chain reaches its contour length. In some cases, such as soft keratins and hagfish slime thread (57,58), intermediate filament-based materials show much lower low strain modulus (a few MPa), but in these cases low stiffness is attributed to the unstructured elastomeric protein matrix connected in series with the stiffer coiled coils.

Only two of these regimes exists in the fibrin fiber stress-strain curve: the soft regime (~1–2 Mpa), and the strain stiffening regime (5–20 Mpa). One possible way the coiled coil hypothesis could be reconciled with a MPa scale modulus is a zipper-type mechanism in which the stress is concentrated rather than distributed throughout the fiber. Only a small fraction of the coiled-coils would bear the total load, and as they unfold, would pass the concentrated load to another isolated fraction of coiled coils. The global stiffness of the fiber would then appear to be much lower than that expected if the load were distributed uniformly. However, we know of no structural data that support nonuniform distribution of the applied load. Therefore, we believe coiled-coil unfolding model to be inconsistent with our data.

Force per monomer

Atomic force microscopy and force spectroscopy studies over the past decade have established the range of forces required to unfold secondary and tertiary protein structure (42,44,59). For protein unfolding to occur within strained fibrin fibers, the resolved forces (per monomer) would have to exceed these thresholds. To address this issue, we present estimates of force per monomer at all strains of fibrin fiber extension (see the Supporting Material for calculation details and assumptions). Fig. 8 shows a plot of fiber force-versus-extension data and corresponding force per monomer (FPM) found by dividing the force by the number of monomers within a fiber cross section. Previous work has shown that the fibrin coiled-coil unfolds at ~100 pN (25,36). Although the FPM in Fig. 8 does cross the threshold for coiled-coil unfolding, it does so at strains well above 100%. In this study, the average fiber strain at the 100-pN FPM threshold value was 130 ± 20% for FXIIIa ligated fibers and 140 ± 20% strain for unligated fibers. Thus, the

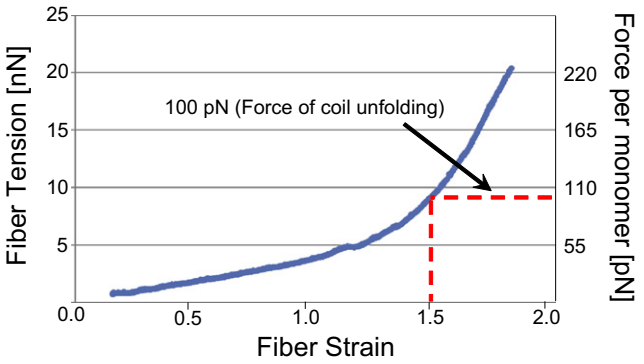

FIGURE 8 Force per monomer as a function of fiber strain.

FPM does not cross the average threshold for coil-unfolding until the fiber is within its strain-stiffening regime. At 50% fiber strain, in the linear fiber regime, the average FPM value was 27 ± 8 pN for ligated fibers and 18 ± 4 pN for unligated fibers, suggesting that coiled-coil unfolding is not a prominent process in the linear strain regime. If extensibility of fibrin up to 50–100% is not mediated by unfolding, it is likely coming from the natively unfolded αC region. We note that in our measurements the local strain rate—which is known to affect measured unfolding forces—is comparable to typical single-molecule force spectroscopy measurements (see Materials and Methods).

Fibrin as elastomeric protein

The persistence length and contour length parameters that emerge from our model fitting, together with the soft (MPa range) elastic modulus, strain stiffening, and high extensibility of individual fibers, present a body of evidence that strongly suggest that the origin of fibrin's mechanical properties lie in the straightening of natively unstructured polypeptides. If this is the case, the tensile elasticity of the fibrin fiber itself is entropic in origin, mediated by straightening of a randomly coiled polypeptide, rather than enthalpic and mediated by straining of chemical bonds within the backbone. The entropic elastic behavior comes not from thermal fluctuations of the fiber segment's overall contour, but from internal degrees of freedom residing in the unstructured peptide sequences within the monomer. The argument has been made in the literature that the architectural parameters for fibrin gels (branch point density in particular) are not consistent with rubberlike elasticity even though fibrin's extensibility and stiffness is comparable to rubber (60,61). This is because unlike in rubbers where very stiff (GPa-scale tensile modulus), very thin, polymer molecules or polypeptides are polymerized into highly cross-linked random coil networks, fibrin gels are made up of thick structurally complex fibers with very low branch point densities. We propose instead that for fibrin, the fibers themselves are rubberlike; the fiber is itself a flexible polymer network.

CONCLUSIONS

Stress-versus-strain evaluation of individual fibrin fibers revealed elastomeric mechanical properties including low modulus (MPa), high extensibility, and strain-stiffening behavior. We found that FXIIIa ligation roughly doubles the stiffness of fibrin both in the low and high strain limit. This underlines a crucial point in fibrin mechanics: in addition to any architectural effects that FXIIIa ligation confers to the overall fibrin network such as fiber diameter and branch point density, it also directly affects individual fiber segment stiffness. We have proposed a mechanical model of the fibrin fiber that describes the observed force-versus-strain behavior. The model depicts the fibrin fiber as a set of parallel chains of monomers linked in series. Each monomer consists of a soft WLC element representing an unstructured region of the fibrin protein monomer. Our force-versus-strain data is fit well by the scaled WLC model and indicates that the unstructured portions of the monomer mediate the mechanical response of fibrin fibers. Our analysis suggests that this unstructured portion is the natively unfolded area of the αC region.

SUPPORTING MATERIAL

Four figures and five equations are available at http://www.biophysj.org/biophysj/supplemental/S0006-3495(10)01056-8.

This work was supported by the National Institutes of Health (grant Nos. HL31048 and P41-EB002025) and the National Science Foundation (grant No. 0705977).

REFERENCES

1. Weisel, J. W. 2004. The mechanical properties of fibrin for basic scientists and clinicians. *Biophys. Chem.* 112:267–276.
2. Hudson, N. E., J. R. Houser, …, M. R. Falvo. 2010. Stiffening of individual fibrin fibers equitably distributes strain and strengthens networks. *Biophys. J.* 98:1632–1640.
3. Liu, W., C. R. Carlisle, …, M. Guthold. 2010. The mechanical properties of single fibrin fibers. *J. Thromb. Haemost.* 8:1030–1036.
4. Falvo, M. R., D. Millard, …, S. T. Lord. 2008. Length of tandem repeats in fibrin's αC region correlates with fiber extensibility. *J. Thromb. Haemost.* 6:1991–1993.
5. Guthold, M., W. Liu, …, S. T. Lord. 2007. A comparison of the mechanical and structural properties of fibrin fibers with other protein fibers. *Cell Biochem. Biophys.* 49:165–181.
6. Liu, W., L. M. Jawerth, …, M. Guthold. 2006. Fibrin fibers have extraordinary extensibility and elasticity. *Science.* 313:634.
7. Kang, H., Q. Wen, …, F. C. Mackintosh. 2009. Nonlinear elasticity of stiff filament networks: strain stiffening, negative normal stress, and filament alignment in fibrin gels. *J. Phys. Chem. B.* 113: 3799–3805.
8. Bale, M. D., and J. D. Ferry. 1988. Strain enhancement of elastic modulus in fine fibrin clots. *Thromb. Res.* 52:565–572.
9. Shah, J. V., and P. A. Janmey. 1997. Strain hardening of fibrin gels and plasma clots. *Rheolog.Acta.* 36:262–268.
10. Janmey, P. A., M. E. McCormick, …, F. C. MacKintosh. 2007. Negative normal stress in semiflexible biopolymer gels. *Nat. Mater.* 6:48–51.

11. Buehler, M. J. 2006. Nature designs tough collagen: explaining the nanostructure of collagen fibrils. *Proc. Natl. Acad. Sci. USA.* 103:12285–12290.
12. Buehler, M. J., and Y. C. Yung. 2009. Deformation and failure of protein materials in physiologically extreme conditions and disease. *Nat. Mater.* 8:175–188.
13. Aizenberg, J., J. C. Weaver, …, P. Fratzl. 2005. Skeleton of *Euplectella* sp.: structural hierarchy from the nanoscale to the macroscale. *Science.* 309:275–278.
14. Lord, S. T. 2007. Fibrinogen and fibrin: scaffold proteins in hemostasis. *Curr. Opin. Hematol.* 14:236–241.
15. Weisel, J. W. 2005. Fibrinogen and fibrin. *Adv. Protein Chem.* 70:247–299.
16. Ferry, J. D., and P. R. Morrison. 1944. Chemical, clinical, and immunological studies on the products of human plasma fractionation. XVI. Fibrin clots, fibrin films, and fibrinogen plastics. *J. Clin. Invest.* 23:566–572.
17. Gerth, C., W. W. Roberts, and J. D. Ferry. 1974. Rheology of fibrin clots. II. Linear viscoelastic behavior in shear creep. *Biophys. Chem.* 2:208–217.
18. Roberts, W. W., O. Kramer, …, J. D. Ferry. 1974. Rheology of fibrin clots. I. Dynamic viscoelastic properties and fluid permeation. *Biophys. Chem.* 1:152–160.
19. Lorand, L. 1950. Fibrin clots. *Nature.* 166:694–695.
20. Roberts, W. W., L. Lorand, and L. F. Mockros. 1973. Viscoelastic properties of fibrin clots. *Biorheology.* 10:29–42.
21. Mockros, L. F., W. W. Roberts, and L. Lorand. 1974. Viscoelastic properties of ligation-inhibited fibrin clots. *Biophys. Chem.* 2:164–169.
22. Ryan, E. A., L. F. Mockros, …, L. Lorand. 1999. Influence of a natural and a synthetic inhibitor of factor XIIIa on fibrin clot rheology. *Biophys. J.* 77:2827–2836.
23. Standeven, K. F., A. M. Carter, …, R. A. Ariëns. 2007. Functional analysis of fibrin gamma-chain cross-linking by activated factor XIII: determination of a cross-linking pattern that maximizes clot stiffness. *Blood.* 110:902–907.
24. Ariëns, R. A., T. S. Lai, …, P. J. Grant. 2002. Role of factor XIII in fibrin clot formation and effects of genetic polymorphisms. *Blood.* 100:743–754.
25. Brown, A. E., R. I. Litvinov, …, J. W. Weisel. 2007. Forced unfolding of coiled-coils in fibrinogen by single-molecule AFM. *Biophys. J.* 92:L39–L41.
26. Lim, B. B., E. H. Lee, …, K. Schulten. 2008. Molecular basis of fibrin clot elasticity. *Structure.* 16:449–459.
27. Averett, L. E., M. H. Schoenfisch, …, O. V. Gorkun. 2009. Kinetics of the multistep rupture of fibrin 'A-a' polymerization interactions measured using atomic force microscopy. *Biophys. J.* 97:2820–2828.
28. Averett, L. E., C. B. Geer, …, M. H. Schoenfisch. 2008. Complexity of "A-a" knob-hole fibrin interaction revealed by atomic force spectroscopy. *Langmuir.* 24:4979–4988.
29. Gosline, J., M. Lillie, …, K. Savage. 2002. Elastic proteins: biological roles and mechanical properties. *Philos. Trans. R. Soc. Lond. B Biol. Sci.* 357:121–132.
30. Gosline, J. M., P. A. Guerette, …, K. N. Savage. 1999. The mechanical design of spider silks: from fibroin sequence to mechanical function. *J. Exp. Biol.* 202:3295–3303.
31. Weisel, J. W. 1986. The electron microscope band pattern of human fibrin: various stains, lateral order, and carbohydrate localization. *J. Ultrastruct. Mol. Struct. Res.* 96:176–188.
32. Tatham, A. S., and P. R. Shewry. 2002. Comparative structures and properties of elastic proteins. *Philos. Trans. R. Soc. Lond. B Biol. Sci.* 357:229–234.
33. Binnie, C. G., and S. T. Lord. 1993. The fibrinogen sequences that interact with thrombin. *Blood.* 81:3186–3192.
34. Gorkun, O. V., Y. I. Veklich, …, S. T. Lord. 1997. The conversion of fibrinogen to fibrin: recombinant fibrinogen typifies plasma fibrinogen. *Blood.* 89:4407–4414.
35. Collet, J. P., H. Shuman, …, J. W. Weisel. 2005. The elasticity of an individual fibrin fiber in a clot. *Proc. Natl. Acad. Sci. USA.* 102:9133–9137.
36. Brown, A. E., R. I. Litvinov, …, J. W. Weisel. 2009. Multiscale mechanics of fibrin polymer: gel stretching with protein unfolding and loss of water. *Science.* 325:741–744.
37. Fowler, W. E., R. R. Hantgan, …, H. P. Erickson. 1981. Structure of the fibrin protofibril. *Proc. Natl. Acad. Sci. USA.* 78:4872–4876.
38. Hantgan, R. R., and J. Hermans. 1979. Assembly of fibrin. A light scattering study. *J. Biol. Chem.* 254:11272–11281.
39. Nelb, G. W., G. W. Kamykowski, and J. D. Ferry. 1980. Kinetics of ligation of fibrin oligomers. *J. Biol. Chem.* 255:6398–6402.
40. Weisel, J. W., Y. Veklich, and O. Gorkun. 1993. The sequence of cleavage of fibrinopeptides from fibrinogen is important for protofibril formation and enhancement of lateral aggregation in fibrin clots. *J. Mol. Biol.* 232:285–297.
41. Kellermayer, M. S., S. B. Smith, …, C. Bustamante. 1997. Folding-unfolding transitions in single titin molecules characterized with laser tweezers. *Science.* 276:1112–1116.
42. Oberhauser, A. F., P. E. Marszalek, …, J. M. Fernandez. 1998. The molecular elasticity of the extracellular matrix protein tenascin. *Nature.* 393:181–185.
43. Rief, M., M. Gautel, …, H. E. Gaub. 1998. The mechanical stability of immunoglobulin and fibronectin III domains in the muscle protein titin measured by atomic force microscopy. *Biophys. J.* 75: 3008–3014.
44. Rief, M., J. Pascual, …, H. E. Gaub. 1999. Single molecule force spectroscopy of spectrin repeats: low unfolding forces in helix bundles. *J. Mol. Biol.* 286:553–561.
45. Schwaiger, I., C. Sattler, …, M. Rief. 2002. The myosin coiled-coil is a truly elastic protein structure. *Nat. Mater.* 1:232–235.
46. Bustamante, C., J. F. Marko, …, S. Smith. 1994. Entropic elasticity of λ-phage DNA. *Science.* 265:1599–1600.
47. Rief, M., M. Gautel, …, H. E. Gaub. 1997. Reversible unfolding of individual titin immunoglobulin domains by AFM. *Science.* 276: 1109–1112.
48. Kellermayer, M. S., C. Bustamante, and H. L. Granzier. 2003. Mechanics and structure of titin oligomers explored with atomic force microscopy. *Biochim. Biophys. Acta.* 1604:105–114.
49. Piechocka, I. K., R. G. Bacabac, …, G. H. Koenderink. 2010. Structural hierarchy governs fibrin gel mechanics. *Biophys. J.* 98: 2281–2289.
50. Sobel, J. H., and M. A. Gawinowicz. 1996. Identification of the α-chain lysine donor sites involved in factor XIIIa fibrin cross-linking. *J. Biol. Chem.* 271:19288–19297.
51. Litvinov, R. I., S. Yakovlev, …, J. W. Weisel. 2007. Direct evidence for specific interactions of the fibrinogen αC-domains with the central E region and with each other. *Biochemistry.* 46:9133–9142.
52. Marko, J. F., and E. D. Siggia. 1995. Statistical mechanics of supercoiled DNA. *Phys. Rev. E.* 52:2912–2938.
53. Miserez, A., S. S. Wasko, …, J. H. Waite. 2009. Non-entropic and reversible long-range deformation of an encapsulating bioelastomer. *Nat. Mater.* 8:910–916.
54. Hearle, J. W. 2000. A critical review of the structural mechanics of wool and hair fibers. *Int. J. Biol. Macromol.* 27:123–138.
55. Qin, Z., L. Kreplak, and M. J. Buehler. 2009. Hierarchical structure controls nanomechanical properties of vimentin intermediate filaments. *PLoS ONE.* 4:e7294.
56. Kreplak, L., and D. Fudge. 2007. Biomechanical properties of intermediate filaments: from tissues to single filaments and back. *Bioessays.* 29:26–35.

57. Fudge, D. S., and J. M. Gosline. 2004. Molecular design of the α-keratin composite: insights from a matrix-free model, hagfish slime threads. *Proc. Biol. Sci.* 271:291–299.

58. Fudge, D. S., K. H. Gardner, …, J. M. Gosline. 2003. The mechanical properties of hydrated intermediate filaments: insights from hagfish slime threads. *Biophys. J.* 85:2015–2027.

59. Rief, M., M. Gautel, and H. E. Gaub. 2000. Unfolding forces of titin and fibronectin domains directly measured by AFM. *Adv. Exp. Med. Biol.* 481:129–141.

60. Ryan, E. A., L. F. Mockros, …, L. Lorand. 1999. Structural origins of fibrin clot rheology. *Biophys. J.* 77:2813–2826.

61. Treloar, L. R. G. 1944. Stress-strain data for vulcanized rubber under various types of deformation. *Trans. Faraday Soc.* 40:59–70.